

# **Statin-activation of RyR1 is a class effect but separable from HMG-CoA reductase inhibition**

Chris Lindsay<sup>1</sup>, Maria Musgaard<sup>3,4</sup>, Angela J. Russell<sup>1,2</sup> & Rebecca Sitsapesan<sup>1\*</sup>

<sup>1</sup> Department of Pharmacology, University of Oxford, UK

<sup>2</sup> Department of Chemistry, Chemistry Research Laboratory, University of Oxford, UK

<sup>3</sup> Structural Bioinformatics and Computational Biochemistry, Department of Biochemistry, University of Oxford, UK.

<sup>4</sup> Present address: OMass Therapeutics, The Schrödinger Building, Heatley Road, The Oxford Science Park, Oxford, OX4 4GE, UK

\*Corresponding author: Rebecca Sitsapesan, Department of Pharmacology, University of Oxford, Mansfield Road, Oxford, OX1 3QT, UK; Tel: +441865271899; Fax: +441865271853; Email: [rebecca.sitsapesan@pharm.ox.ac.uk](mailto:rebecca.sitsapesan@pharm.ox.ac.uk)

**Running title:** RyR1 activation is a class effect of statins

## **Abstract**

### **Background and purpose**

Statins, inhibitors of HMG-CoA reductase, are mainstay treatment for hypercholesterolemia. However, muscle pain and weakness prevent many patients from benefiting from their cardioprotective effects. We previously demonstrated that simvastatin activates skeletal ryanodine receptors (RyR1), an effect that could be important in initiating myopathy. We therefore investigated if RyR1 activation is a standard property of commonly-prescribed statins. Using a range of structurally-diverse statin analogues we examined structural features associated with RyR1 activation, aiming to identify statins lacking this property.

### **Experimental Approach**

Compounds were screened for RyR1 activity utilising [<sup>3</sup>H]ryanodine binding. Mechanistic insight into RyR1 activity was studied by incorporating RyR1 channels from sheep, mouse or rabbit skeletal muscle into bilayers.

### **Key Results**

All UK-prescribed statins activated RyR1 at nanomolar concentrations. Cerivastatin, withdrawn from the market due to life-threatening muscle-related side effects, was more effective than currently-prescribed statins and possessed the unique ability to open RyR1 channels independently of cytosolic Ca<sup>2+</sup>. We synthesised the minimal statin pharmacophore and it did not activate RyR1. We also identified five analogues retaining potent HMG-CoA reductase inhibition that inhibited RyR1 and four analogues that lacked the ability to activate RyR1.

## Conclusion and Implications

That cervistatin activates RyR1 most strongly supports the hypothesis that RyR1 activation is implicated in statin-induced myopathy. Demonstrating that statin-regulation of RyR1 and HMG-CoA reductase are separable effects will allow the role of RyR1 in statin-induced myopathy to be further elucidated by the tool compounds we have identified, thus paving the way for the development of effective cardioprotective statins with improved patient tolerance.

**Keywords:** statin, ryanodine receptor, RyR1, myopathy, single-channel,  $\text{Ca}^{2+}$ -release

**Abbreviations:** HMG-CoA, 3-hydroxy-3-methylglutaryl CoA; LDL, low density lipoprotein; MH, malignant hyperthermia; CCD, central core disease.

### What is already known

- Simvastatin activates single RyR1 channels and increases sarcoplasmic reticulum (SR)  $\text{Ca}^{2+}$ -release in muscle cells.
- Inappropriate SR  $\text{Ca}^{2+}$ -release has known association with myopathy and rhabdomyolysis, both side effects of statins.

### What this study adds

- RyR1 activation is a class effect of all commonly-prescribed statins. Cerivastatin is particularly effective.
- Potent HMG-CoA inhibition is achievable without also activating RyR1.

### What is the clinical significance

- Cerivastatin, which caused the most dangerous patient side effects, exhibits greater ability to activate RyR1
- The development of statins that do not activate RyR1 may allow many more patients to benefit from their lipid-lowering effects.

## Introduction

Statins are amongst the most widely prescribed drugs worldwide, as treatment for both the primary and secondary prevention of cardiovascular events (Oates et al., 1988; Nishimura et al., 2014). Global sales are soon predicted to reach \$1 trillion, while atorvastatin was the most widely prescribed drug in the UK in 2018, with over 37% of the adult population eligible for treatment (Ioannidis, 2014; Ueda et al., 2017). Statins are prescribed to reduce blood cholesterol levels and the mechanism of action of all statins relies on competitive inhibition of the enzyme catalysing the rate-determining step of cholesterol synthesis, HMG-CoA reductase. The decrease in cholesterol production also promotes the redirection of cholesterol to the liver via low density lipoprotein cholesterol (LDL) receptors, thus further lowering plasma cholesterol levels (Brown and Goldstein, 2004). Large scale clinical trials have demonstrated that statins can promote up to 60% reductions in plasma LDL levels, and have shown that their use is associated with a significant decrease in the risk of cardiovascular events (Vaughan and Gotto, 2004; Collins et al., 2016).

There are currently five statins prescribed in the United Kingdom: atorvastatin (Lipitor), simvastatin (Zocor), pravastatin (Lipostat), fluvastatin (Lescol) and rosuvastatin (Crestor). They can be broadly grouped into two categories based on their chemical structures; those based upon a natural product decalin core (e.g. simvastatin), and those which are based upon a fully synthetic polycyclic structure (e.g. atorvastatin) (Istvan, 2003). However, while structurally distinct, all statins share the same basic interactions with HMG-CoA reductase (Schachter, 2005). They all contain a common pharmacophore, a 3,5-dihydroxyhept-6-enoic acid unit, which mimics HMG-CoA and hence occupies the same binding site of HMG-CoA reductase as its natural substrate (Istvan and Deisenhofer, 2001). This pharmacophore interconverts *in vivo* between an open salt/acid form and a ring-closed lactone form (Figure 1A, inset) in a process that depends strongly on pH (Taha et al., 2016).

Despite their proven efficacy in lowering plasma cholesterol levels, not all patients can tolerate the dose of statins required to achieve a therapeutic benefit (Ward et al., 2019). This can be due to skeletal muscle related side effects which are an established feature of statin treatment. These include myalgias/muscle pain, myopathy linked to a rise in creatine kinase, and, in very severe cases, rhabdomyolysis which can result in death (Tomaszewski et al., 2011). The exact prevalence of statin side effects is a matter of debate, as controlled placebo-based trials have reported incidence levels for myopathy of between 1-10%, while observational studies report

values as high as 30% (Bruckert et al., 2005; Parker et al., 2013; Adhyaru and Jacobson, 2018). There is also significant evidence that the co-administration of drugs such as gemfibrozil can increase plasma statin concentration and increase the risk of adverse effects (Jacobson and Zimmerman, 2006). The most serious cases of rhabdomyolysis appear to occur in approximately 1 in 10,000 patients on statin treatment (Newman and Tobert, 2018). The most adverse effects occurred with cerivastatin (Baycol), a statin withdrawn from the market in 2001, as postmarket surveillance reported 52 deaths had occurred from rhabdomyolysis as a result of its use (Furberg and Pitt, 2001). While it is fortunate that the majority of reported side effects are mild, there is significant evidence that they result in a decrease in patient adherence to medication, reducing the effectiveness of statins in the clinical setting (Mann et al., 2010).

The core driver of statin side effects has been the subject of intense research, with a number of proposed mechanisms. These include disruption of mitochondrial respiration (Dohlmann et al., 2019), depletion of coenzyme Q<sub>10</sub> levels (Deichmann et al., 2010), reduction of cellular structural integrity (Draeger et al., 2006) and reduced levels of downstream metabolites such as farnesyl pyrophosphate (Abd and Jacobson, 2011). However, although muscle-related side-effects are associated with all statins, their severity or incidence does not appear to correlate with relative ability to inhibit HMG-CoA reductase, suggesting that they must be caused by a mechanism independent from cholesterol depletion (Armitage, 2007). It instead appears that the disruption of Ca<sup>2+</sup> signalling in skeletal muscle cells may be important. It is well established that muscle contraction relies on a coordinated cycling of Ca<sup>2+</sup> release and re-uptake from the sarcoplasmic reticulum (SR) (Rios and Brum, 1987; Gordon et al., 2000). Statins have been found to interrupt this cycle by provoking inappropriate Ca<sup>2+</sup>-release from the SR. Acute treatment triggers large Ca<sup>2+</sup>-release from the SR both in individual rat SR vesicles (Inoue et al., 2003b) and in whole muscle fibres (Sirvent et al., 2005), while chronic statin treatment in rats appears to increase the resting Ca<sup>2+</sup> concentration ([Ca<sup>2+</sup>]<sub>i</sub>) in muscle cells (Liantonio et al., 2007). It had been suggested that statins could operate via the skeletal muscle ryanodine receptor (RyR1), the main SR Ca<sup>2+</sup>-release channel in skeletal muscle), and we recently reported that this is indeed the case ((Sirvent et al., 2005; Venturi et al., 2018). We showed that simvastatin directly activates single skeletal muscle RyR1 channels incorporated into artificial membranes under voltage clamp conditions (Venturi et al., 2018). Simvastatin also stimulated the binding of [<sup>3</sup>H]ryanodine to RyR1, demonstrating that populations of RyR1 channels in their native membranes are also activated by this statin (Venturi et al., 2018).

Given the association between RyR1 dysfunction, myopathy, and statin-induced  $\text{Ca}^{2+}$ -release, we hypothesised that statin-induced RyR1 activation is a contributing factor to the muscle-related side effects of patients prescribed statin treatment (Lindsay, 2018; Venturi et al., 2018). We now report that RyR1 activation is a class effect, common to all statin drugs currently approved for use in the UK. We further describe the identification of statin molecules, structural analogues of atorvastatin, which are devoid of RyR1 activation, as tool compounds to inform the development of the next generation of statin drugs.

## Methods

### *Animals and ethical approval*

Single-channel experiments were performed using either mouse, rabbit or sheep skeletal or cardiac muscle tissue as indicated in individual figure legends. All [ $^3\text{H}$ ]ryanodine binding experiments were performed using tissue derived from sheep. Tissue derived from sheep was obtained from an abattoir and transported to the laboratory in cardioplegic solution at 4°C. Sheep were Suffolk breed, aged between 8-10 years, and of mixed sex. Rabbit skeletal muscle tissue was obtained from New Zealand breed animals which were obtained from a commercial supplier. Mice were housed in a specific pathogen-free unit in individually ventilated cages on a 12 h light/dark cycle with free access to food and water. In all cases, tissue was derived from animals which had been sacrificed for other purposes, in order to minimise the number of animals used in compliance with the principles of the ‘three Rs’. All rodent work was performed in accordance with the Directive 2010/63/EU of the European Parliament with local approval of the Animal Research Committee according to the regulations on animal experimentation at the University of Oxford (mouse).

### *Preparation of SR vesicles*

Heavy sarcoplasmic reticulum (HSR) vesicles were prepared from skeletal (RyR1) or cardiac (RyR2) muscle tissue as previously reported (Sitsapasan and Williams, 1990).

### *Single-channel recordings*

Skeletal or cardiac HSR vesicles were incorporated into planar phospholipid bilayers as previously described (Sitsapasan et al., 1991). Voltage-clamp conditions were used to measure the current through the RyR channels, with the *trans* (luminal) chamber voltage-clamped at ground. The recording solutions used were 250 mM HEPES, 80 mM Tris, 10  $\mu\text{M}$  free  $\text{Ca}^{2+}$ ,

pH 7.2 on the cytosolic side and 250 mM glutamic acid, 10 mM HEPES,  $\approx$  50 mM free  $\text{Ca}^{2+}$  on the luminal side; both at 21°C. The statin compound under investigation was added to the cytosolic or luminal chamber as required. The free  $[\text{Ca}^{2+}]$  was maintained by the addition of EGTA and  $\text{CaCl}_2$  solution and measured using a Orion 93-20  $\text{Ca}^{2+}$  electrode (Thermo Fisher Scientific, UK) as previously described (Sitsapasan et al., 1991). The pH of solutions was determined using a Ross-type pH electrode (Orion 81-55, Thermo Fisher Scientific, UK) as previously described (Sitsapasan et al., 1991). To lower free cytosolic  $[\text{Ca}^{2+}]$  below subactivating levels, 1 mM EGTA was added. This reduced free  $[\text{Ca}^{2+}]$  below measureable levels and the concentration was calculated using the MaxChelator programme (<http://maxchelator.stanford.edu>) (Stanford, USA) to  $< 1$  nM.

### ***Single-channel analysis***

Single-channel analysis was performed as described previously (Sitsapasan and Williams, 1990; Sitsapasan et al., 1991). Briefly, recordings were low-pass filtered at 800 Hz and digitized at 20 kHz. Open probability ( $P_o$ ) was determined over 3 min of continuous recording, and this is the value reported in all figures. Where several channels were present in a recording, the average  $P_o$  based on  $N$  channels is reported according to the equation:

$$\text{average } P_o = \frac{NP_o}{N} = \frac{P_{o1} + P_{o2} + P_{o3} + \dots + nP_{on}}{N}$$

Where  $P_{o1}$ ,  $P_{o2}$  and  $P_{o3}$  are the probability of dwelling in the first, second or third channel level respectively. Lifetime analysis was performed when only one channel was present in the bilayer using Clampfit 10.6 (Molecular Devices, USA).

### ***[ $^3\text{H}$ ]ryanodine binding***

HSR vesicles (100-130  $\mu\text{g}/\mu\text{l}$ ) were incubated at 37°C in 250 mM HEPES, 80 mM Tris, 10  $\mu\text{M}$  free  $\text{Ca}^{2+}$ , pH 7.2, 5 nM [ $^3\text{H}$ ]ryanodine for 90 min. Samples were filtered through glass 25 mm diameter microfibre filters (VMR, UK) and the filters were washed with 10 ml of ice-cold water. The filters were dissolved in 20 mL of scintillation fluid (EmulsiferSafe, Perkin Elmer, UK) and counted. Nonspecific binding was determined from a sample with an additional 5  $\mu\text{M}$  unlabelled ryanodine added. All experiments were performed in triplicate.

### ***Data and statistical analysis***

The data and statistical analysis in this study comply with the recommendations on experimental design and analysis in pharmacology (Curtis et al., 2015). Data analysis was

performed using Graphpad Prism 7 (San Diego, California USA). Data were assessed for normality using the D'agostino and Pearson test. Data are expressed as mean  $\pm$  SEM, and where  $n \geq 5$ , comparisons are made using Student's *t*-test. A *p* value of  $< 0.05$  was taken as significant throughout. Variations in *n* numbers reported for single-channel experiments are due to bilayers breaking during the experiment, precluding further measurements being taken. In all cases, data were obtained from at least five different skeletal and cardiac membrane preparations (using tissue derived from one animal each for sheep and five animals for mouse). With the exception of the data presented in Figure 5, single-channel analysis could not be blinded to treatment groups due to the large and unmistakable effect of statin drugs on the RyR.. To control for variation between SR preparations, [<sup>3</sup>H]ryanodine binding data was normalised relative to control binding levels (250 mM HEPES, 80 mM Tris, 10  $\mu$ M free Ca<sup>2+</sup>, pH 7.2). No outlier analysis was performed and no data was excluded from analysis.

## **Materials**

Statin sodium salts were obtained from CarboSynth Ltd (Compton, UK). [9, 21(n)-<sup>3</sup>H]ryanodine was obtained from Amersham Biosciences (Buckinghamshire, UK). All other chemicals were purchased from Sigma-Aldrich (Dorset, UK) or VWR (Poole, UK). The atorvastatin analogues in Figure 7 were kindly provided by *Pfizer inc* via their compound transfer program. Water was deionised (Millipore, Harrow, UK) and all single channel recording solutions were filtered through a membrane of 0.45  $\mu$ M diameter before use.

## **Results**

### ***All commonly prescribed statins activate RyR1***

[<sup>3</sup>H]ryanodine binding can be used to estimate the Po of populations of RyR channels in their native membranes (Lindsay et al., 2018). The statins, which are currently prescribed in the UK (Figure 1A), as well as cerivastatin, were therefore investigated for their ability to stimulate [<sup>3</sup>H]ryanodine binding to skeletal HSR vesicles containing RyR1 (Figure 1A). It was found that all of these statins increased [<sup>3</sup>H]ryanodine binding at similar nanomolar concentrations, indicating that they may bind to RyR1 with similar affinity (Figure 1B). Cerivastatin, which was removed from the market due to adverse effects (Maggini et al., 2004) was more effective than the other statins, causing the highest maximum level of [<sup>3</sup>H]ryanodine binding (Figure 1B).

### *Atorvastatin and Cerivastatin activate single RyR1 channels*

[<sup>3</sup>H]ryanodine binding can provide an estimate of the activity of a population of RyR channels but single-channel analysis is required to investigate the mechanism of action of drugs and to exclude the possibility that a drug could directly affect the interaction of ryanodine with its binding site on RyR (Laver, 2001). We therefore incorporated sheep heavy SR vesicles containing RyR1 channels into planar lipid bilayers under voltage-clamp conditions. Atorvastatin and cerivastatin were selected for single-channel experiments, as atorvastatin is the most widely prescribed among the available drugs, while cerivastatin caused fatalities in the patient population (Furberg and Pitt, 2001) and, in the above [<sup>3</sup>H]ryanodine binding assay, appeared to be the strongest activator of RyR1. In the presence of 10  $\mu$ M free cytosolic  $\text{Ca}^{2+}$ , both statins caused a concentration-dependent increase in  $P_o$  when added to the cytosolic chamber as shown in the representative experiments (Figure 2A and B). The comparative single-channel traces demonstrate that cerivastatin is more effective at each concentration tested, and this is confirmed in the concentration-response relationships shown in Figure 2C. It is clear that both statins are partial agonists, but that cerivastatin has a greater ability (efficacy) to increase  $P_o$  to high levels. As the example traces show, activation by both statins was reversible when control conditions were restored by perfusion, although a longer perfusion time was required to remove cerivastatin (3 min vs 2 min for atorvastatin). This may suggest that cerivastatin dissociates slower from RyR1 or reflect its greater tendency to partition into membranes (Galiullina et al., 2019). After perfusion,  $P_o$  was  $0.0138 \pm 0.0072$ ;  $n=6$ , and  $0.0138 \pm 0.0073$ ;  $n = 5$  for atorvastatin and cerivastatin, respectively.

Addition of atorvastatin to the luminal chamber did not cause a significant increase in  $P_o$ , even at high concentrations, (control  $P_o$ :  $0.0295 \pm 0.0075$ ; 100  $\mu$ M luminal atorvastatin:  $0.0318 \pm 0.0128$ ). A similar observation was found with simvastatin (Venturi et al., 2018).

We also investigated whether there were any marked species differences in the ability of statins to activate RyR1. Atorvastatin increased the  $P_o$  of single RyR1 channels derived from sheep, mouse and rabbit skeletal muscle to similar levels (Figure 2D). This is consistent with the high level of similarity in the RyR1 gene between these species (Hakamata et al., 1992).

We have previously demonstrated that activation of RyR channels by simvastatin is  $\text{Ca}^{2+}$ -dependent, requiring the presence of cytosolic  $\text{Ca}^{2+}$  for maximum effectiveness (Venturi et al., 2018). We therefore investigated if activation of RyR1 by atorvastatin and cerivastatin was also dependent on cytosolic  $\text{Ca}^{2+}$ . Figure 3(A and B) shows typical experiments where the



cytosolic free  $[Ca^{2+}]$  was lowered to a sub-activating level ( $< 1\text{ nM}$ ) to abolish channel openings (top traces). Under these conditions, the figure shows that subsequent additions of low nanomolar concentrations of cerivastatin can still induce channel openings whereas high micromolar levels of atorvastatin are required to produce any activation. The mean open time under these conditions with  $100\text{ nM}$  cerivastatin was  $1.95 \pm 0.34\text{ ms}$  ( $n = 4$ ) compared to  $0.82 \pm 0.29\text{ ms}$  ( $n = 7$ ) ( $p < 0.05$ ) with  $10\text{ }\mu\text{M}$   $Ca^{2+}$  as sole activator, showing that these  $Ca^{2+}$ -independent openings are longer than the  $Ca^{2+}$ -dependent openings observed in the presence of activating cytosolic  $[Ca^{2+}]$ . This is consistent with the  $Ca^{2+}$ -independent gating observed with other effective RyR activators such as caffeine and ATP (Sitsapesan and Williams, 1990; Kermode et al., 1998; Venturi et al., 2018). The ability of low nanomolar concentrations of cerivastatin to activate RyR1 at sub-activating levels of cytosolic  $Ca^{2+}$  could be a property that increases the likelihood of leaking excess  $Ca^{2+}$  from skeletal muscle SR at rest. To understand the relative potentiation of RyR1 channel openings that cerivastatin causes at sub-activating  $[Ca^{2+}]$  ( $< 1\text{ nM}$ ), at the resting free  $[Ca^{2+}]$  in a cell ( $100\text{ nM}$ ), and during a  $Ca^{2+}$ -release event ( $10\text{ }\mu\text{M}$ ), we compared the effects of a low concentration of cerivastatin ( $100\text{ nM}$ ) at these free  $[Ca^{2+}]$  as shown in Figure 3C. It can be seen that at the cellular resting free  $[Ca^{2+}]$  of  $100\text{ nM}$ , cerivastatin is capable of promoting significant channel activation but that the magnitude of activation becomes greater with increasing levels of cytosolic  $Ca^{2+}$ . This potent effect of cerivastatin could be responsible for the disruption to muscle  $Ca^{2+}$  homeostasis that has been reported in patients (Inoue et al., 2003a). If this is the case, then it is important to ascertain if cerivastatin still induces RyR1 openings at resting free  $[Ca^{2+}]$  of  $100\text{ nM}$  in the presence of the physiological regulators, ATP and Mg. Figure. 3D shows a representative experiment performed in the presence of  $100\text{ nM}$  free cytosolic  $Ca^{2+}$ ,  $1\text{ mM}$  free cytosolic  $Mg^{2+}$  and  $5\text{ mM}$  ATP. The top trace shows channel gating under these control conditions. It can be seen that cerivastatin produced a concentration-dependent increase in Po. Figure. 3E shows the mean data illustrating the potent nature of the activation by cerivastatin.

### ***RyR1 activation is not related to HMG-CoA reductase inhibition***

If the goal of producing a HMG-CoA reductase inhibitor that lacks the ability to activate RyR1 is to be successful, it is vital that the HMG-CoA reductase pharmacophore itself does not give rise to activation. To confirm this, the statin minimal pharmacophore, common between all statins (Figure 4A) was synthesised and investigated for its ability to alter RyR1 gating. The statin minimal pharmacophore (**R**)-**1** consists of a five carbon hydroxyglutaric acid component, and may interconvert between closed lactone and open salt/acid forms (Figure 4A). (*R*)-**1** and

its corresponding sodium salt were synthesised according to a modified procedure based upon that previously reported by Loubinoux and colleagues (Loubinoux et al., 1995)(Figure 4B).

The aldehyde **4** was prepared by TBDPS protection of propane-1,3-diol **2** followed by Swern oxidation in 64% yield over two steps, using previously published procedures (Raghavan and Samanta, 2013). Subsequent Evans aldol reaction with oxazolidinone **5** afforded a mixture of diastereomers **6** and **7** in the ratio of 1.65 : 1 and overall yield of 61%. The low selectivity of this method when utilising isopropyl-substituted oxazolidinones has been previously reported (Yamashita et al., 2018), however, the resulting diastereomers could be easily separated by flash column chromatography. Subsequent treatment with HF in pyridine afforded the unprotected diastereomers **8** and **9** in good yield. Finally, treatment with Et<sub>3</sub>N for 48 hours and subsequent co-evaporation with toluene yielded the target minimal pharmacophore (*R*)-**1** and its enantiomer (*S*)-**1**. The absolute configuration of each was confirmed by use of a chiral shift reagent and by comparison to the literature where the configuration was unambiguously determined (Loubinoux et al., 1995). Access to their corresponding sodium salts was achieved by addition of NaOH to pH 7.4, followed by overnight incubation at 37°C, after which LC-MS indicated full conversion.

Figure 4C demonstrates that neither (*R*)-**1**, (*S*)-**1**, nor their sodium salts significantly stimulated the binding of [<sup>3</sup>H]ryanodine to HSR vesicles at concentrations up to 1 mM, indicating that the statin pharmacophore does not, alone, activate RyR1. To emphasise this point, the cerivastatin data from Figure 1B is plotted on the graph to illustrate the degree to which cerivastatin stimulates [<sup>3</sup>H]ryanodine binding under these conditions.

### ***Discovery of statins devoid of RyR1 activation***

Following this finding, we undertook to identify a statin molecule which retained the ability to potently inhibit HMG-CoA reductase while having no effect on RyR1 ion-channel function. Hence, a variety of atorvastatin analogues were investigated for their ability to activate RyR1. These were kindly provided by Pfizer (East 42<sup>nd</sup> Street, New York, 10017), and were based upon Pfizer's previously reported atorvastatin analogue 'inhibitor 2' (**P1**, Figure 5A), which differs from atorvastatin through transposition of the pharmacophore to the nitrogen atom of the pyrrole, and the addition of a second fluoro group as shown in Figure 5A) (Pfefferkorn et al., 2007b). The analogues were selected for their structural diversity, and all feature modifications to the hydrophobic region of the atorvastatin molecule, with either bulky or polar groups. We define the hydrophobic region to include both the amide and fluorophenyl

substituents of atorvastatin. The chemical structures are shown in Figure 5A. These can be broadly categorised into four series based on their structures: (1) anilide series (**P1** to **P10**); (2) conformational restriction (**P11**); (3) pyridine substituted (**P12** to **P13**) and (3) sulfamoyl pyrroles (**P14** to **P16**).

The synthesis of these analogues has been previously reported and the experimentally determined HMG-CoA IC<sub>50</sub> value is available for each molecule. All those included in this study had an HMG-CoA IC<sub>50</sub> value lower than 15 nM and hence have proven to be potent statin molecules (Pfefferkorn et al., 2007b). The majority have additionally had this activity confirmed *in vivo* via a reduction in mouse cholesterol synthesis (Suzuki et al., 2001; Bratton et al., 2007; Larsen et al., 2007; Pfefferkorn et al., 2007b, 2007a; Park et al., 2008).

The analogues were subsequently investigated for their experimental ability to influence RyR1 activity, by examining their ability to stimulate [<sup>3</sup>H]ryanodine binding to skeletal HSR. As shown in Figure 5B, of the 16 compounds investigated, at the concentration of 100 nM, seven stimulated (indicating RyR1 activation) and five inhibited (indicating RyR1 inhibition) [<sup>3</sup>H]ryanodine binding. The figure also shows how the ability of atorvastatin and cerivastatin to stimulate or inhibit [<sup>3</sup>H]ryanodine binding at 100 nM compares with that of the 16 compounds. For the compounds that stimulated or inhibited [<sup>3</sup>H]ryanodine binding, we investigated the effects of two higher concentrations and the effects of these are shown in Figures 5C and 5D. Four compounds did not influence [<sup>3</sup>H]ryanodine binding even at concentrations as high as 10 µM as shown in Figure 5D. The effects of cerivastatin (from Figure 1B) are shown to highlight the lack of effect of these compounds.

## Discussion

Despite the wide-spread use of statin drugs, a clear explanation for their muscle-related side effects has not yet been established (Ward et al., 2019). We have previously reported that simvastatin both significantly and reversibly increased RyR1 Po and suggested that this activation may contribute to the adverse effects of statins, given the crucial role of RyR channels in maintaining cellular Ca<sup>2+</sup> homeostasis and the pleiotropic consequences of disturbed Ca<sup>2+</sup> signalling for muscle function (Venturi et al., 2018). In this study, we now find that all statins routinely prescribed in the United Kingdom are RyR1 activators and that this can be considered a class effect of statins. Two statins, atorvastatin and cerivastatin, were selected for more detailed investigation, representing statins with low and high prevalence of

side effects, respectively (Newman et al., 2019). Cerivastatin was removed from the market due to rhabdomyolysis that resulted in 52 deaths (Furberg and Pitt, 2001) and therefore provides an excellent vehicle to understand the effects of statins on RyR1 channels.

We found that both atorvastatin and cerivastatin increased the  $P_o$  of RyR1 channels incorporated into planar lipid bilayers, and that this effect was concentration dependent and reversible, as previously observed for simvastatin (Venturi et al., 2018). This effect also appeared to be independent of the species from which the RyR1 channels were derived, with mouse, rabbit and sheep RyR1 displaying similar levels of activation (Figure 2D). Lifetime analysis of single-channel events revealed that both statins also share the mechanism of activation previously identified for simvastatin. That is, binding primarily to the closed state of the channel and raising RyR1  $P_o$  by increasing the frequency of channel openings. This mechanism is also how cytosolic  $Ca^{2+}$  regulates RyR1, suggesting that the binding of statins to RyR1 increases the sensitivity of the channel to  $[Ca^{2+}]$ . This is supported by the observation that reducing free cytosolic  $[Ca^{2+}]$  to sub-activating levels with EGTA abolishes statin-induced channel openings. In the case of atorvastatin, some  $Ca^{2+}$ -independent openings could be induced by high concentrations (100  $\mu M$ ) of statin but only very low  $P_o$  values could be achieved. On the contrary, even low concentrations of cerivastatin (10 nM) were able to open the channels at sub-activating cytosolic  $[Ca^{2+}]$ . Importantly, 10 nM cerivastatin could also significantly activate RyR1 at physiological resting free  $[Ca^{2+}]$  (100 nM) in the presence of the key physiological RyR1 regulators,  $Mg^{2+}$  and ATP. Excess RyR1  $Ca^{2+}$ -leak at rest is a well-established phenomenon associated with disease states such as central core disease and malignant hyperthermia (Kushnir et al., 2020). Thus, these powerful agonistic effects of cerivastatin on RyR1 are especially noteworthy, given that that cerivastatin was withdrawn from the market. Cerivastatin, compared to other statins, most effectively stimulated the binding of  $[^3H]$ ryanodine to isolated SR vesicles, in line with having the greatest ability to increase the  $P_o$  of individual RyR1 channels. If, as we suggest, RyR1 dysfunction initiates the intracellular changes that lead to statin-induced myopathy, then we would indeed expect the side-effects of cerivastatin to be the most severe of the clinically relevant statins. The exact correlation between RyR1 activation and propensity for muscular side effects will also depend on other additional factors, such as the lipophilicity of the statin drug in question, as more lipid-soluble statins such as cerivastatin have also been shown to penetrate the muscle to a greater extent (Schachter, 2005; Fong, 2014). However, the finding that cerivastatin is the strongest activator of RyR, at all cytosolic  $[Ca^{2+}]$ , including sub-activating levels, supports the

hypothesis that inappropriate activation of RyR1 may be the first step leading to statin-induced myopathy.

The single-channel methods employed in this study allow the exact concentration of statin in the vicinity of RyR1 to be tightly controlled, an advantage over cellular experiments that rely on a drug to cross cellular membranes. However, in order to fully understand the effects of statins on skeletal muscle, we must determine what concentration of statin the RyR channels may be exposed to in a clinical setting. Others have noted their concern that reports of the effects of statins on various cell proteins / systems by other authors utilised supraclinical concentrations of statins, often into the high micromolar or millimolar range (Bjorkhem-Bergman et al., 2011). Indeed, the plasma concentrations of statins is generally low. For nearly all statins high plasma protein affinity reduces the 'free' concentration further (Stern et al., 2000). In the case of atorvastatin, steady state plasma concentrations have been found to be approximately 4 nM and 10 nM for 20 mg and 80 mg dosing regimens respectively (DeGorter et al., 2013). What is not always appreciated though, is the finding that statins accumulate in the muscles of human patients to hundreds of times their plasma concentrations, an effect predominately driven by active transporters such as the organic anion transporter OATP2B1 (Knauer et al., 2010; Schirris et al., 2015). This also explains why statins are effective despite the fact that their IC<sub>50</sub> values for HMG-CoA reductase range from approximately 5 nM to 44 nM (McKenney, 2003), many times their plasma concentrations. In light of this, we therefore focused on statin concentrations in the 10-100 nM range to most accurately reflect the likely concentrations of statins that accumulate inside the skeletal muscle cells. The fact that we found atorvastatin and cerivastatin to cause significant activation at these concentrations further supports the likelihood that increased RyR1 activation in statin users is clinically relevant.

Having found that all commonly prescribed statins are agonists of RyR1, we investigated if this was an activity shared by all competitive inhibitors of HMG-CoA reductase. If undesired RyR1 activation gives rise to statin myopathy, the design of new statin drugs with reduced side effects would require that the functional groups of the molecule which cause RyR1 activation can be removed without disturbing its affinity for HMG-CoA reductase. To investigate this, the statin minimal pharmacophore (*R*)-**1** was synthesised and examined for its ability to activate RyR1 (Figure 4). Both the open and closed ring forms of the pharmacophore were found to have no effect on RyR1 activity at concentrations up to 1 mM, suggesting that the statin pharmacophore is not, on its own, the motif responsible for binding to RyR1. This suggested that it may be possible for a molecule to be a potent inhibitor of HMG-CoA reductase while

lacking RyR1 activity. We extended this finding by screening a structurally diverse collection of atorvastatin analogues for RyR1 activity, and identified four analogues that were potent inhibitors of HMG-CoA reductase ( $IC_{50} < 2$  nM) and which did not activate or inhibit RyR1 at concentrations which are many times greater than that required to provide the desired inhibition of HMG-CoA reductase. Concentrations as high as 1 mM did not influence RyR1 activity and this is approximately  $10^6$  times greater than the HMG-CoA  $IC_{50}$  for compounds **P1**, **P5**, **P6** and **P8** (1.8 nM, 0.2 nM, 0.3 nM and 0.8 nM respectively) (Pfefferkorn et al., 2007b). For comparison, atorvastatin and cerivastatin already activate RyR1 to an extent at concentrations equal to their HMG-CoA  $IC_{50}$  (8-10 nM) (Figure 2). Importantly, these analogues have already been shown to possess *in vivo* cholesterol-lowering effects, as well as an acceptable safety profile (Suzuki et al., 2001; Bratton et al., 2007; Larsen et al., 2007; Pfefferkorn et al., 2007b, 2007a; Park et al., 2008). These compounds therefore demonstrate that RyR1 activation is not a property dooming all statins but is a separate and surmountable obstacle.

Our results have indicated several structural features of statin molecules that may drive activation and inhibition of RyR1. These features are summarised in Figure 6B. Principally, it appears that compounds possessing a small polar functionality at C(5) of the pyrrole (**P12**, cyano and **P13**, aminocarbonyl) appeared to be the activators of RyR1, including an example where the amide was cyclised onto the adjacent aryl substituent at C(4). Conversely, the three compounds that possess a 5-sulfamoyl pyrrole motif (**P14**, **P15**, **P16**) were uniformly inhibitors, with all three reducing [ $^3$ H]ryanodine binding to around 50% of control levels. Analogues with small groups at C(5) of the pyrrole such as ethyl or cyclopropyl groups (**P9** and **P10**) were also inhibitors. However, the most important finding of this work has been the identification of compounds which are inactive against RyR1, and, in this regard, it is conspicuous that all of the inactive compounds (**P1**, **P5**, **P6** and **P8**) have in common a C(5) aryl ring, although further structure-activity-relationship analyses will be required to understand which substituents and regiochemistry are critical to avoid RyR1 activation. This suggests that it may be this functionality that is important for reducing a compound's ability to bind to or activate the channel, and other groups such as the 4-sulfamoyl pyrrole can bind more easily. Importantly, these inactive compounds retain the functionality required for binding to HMG-CoA reductase, including the statin pharmacophore and the 4-fluorophenyl group. While further studies will be required to understand the cause of this structure-activity relationship, these trends represent important new information for the development of new RyR1 inactive statin compounds.

In summary, we have demonstrated that all clinically-used statins in the UK are potent partial agonists of RyR1, capable of increasing the Po of RyR1. This could be an initiating factor in statin-induced myopathy. We show that cerivastatin additionally possesses a unique ability to activate RyR1 in the absence of activating levels of cytosolic  $[Ca^{2+}]$ , making the channel more likely to leak excess SR  $Ca^{2+}$  at rest, causing patients to be at increased risk of rhabdomyolysis and death. We have also identified potent inhibitors of HMG-CoA reductase that can inhibit RyR1 or, importantly, do not modulate RyR1 Po at all. This crucial finding, that statin-modulation of RyR1 and HMG-CoA are clearly separable effects, will facilitate the development of novel statin compounds that do not target RyR1, thus reducing the likelihood of dysfunctional muscle  $Ca^{2+}$ -handling. With increasing numbers of patients becoming eligible for statin therapy, it is more important than ever to facilitate the development of next-generation statins that will allow more patients to benefit from their cardioprotective effects.

### **Competing Interests**

The authors declare no competing financial interests.

### **Author Contribution**

C.L. performed the experiments and analysed the data. All authors conceived and designed the study, wrote the manuscript, discussed the results and critiqued the manuscript for intellectual content.

### **Funding**

This work was supported by the British Heart Foundation (PG/19/38/34403). R. S. and A. J. R. acknowledge support from the British Heart Foundation Centre of Research Excellence, Oxford (RE/08/004) through the provision of a studentship (to C.L.)

### **References**

- Abd, T.T., and Jacobson, T.A. (2011). Statin-induced myopathy: A review and update. *Expert Opin. Drug Saf.* 10: 373–387.
- Adhyaru, B.B., and Jacobson, T.A. (2018). Safety and efficacy of statin therapy. *Nat. Rev. Cardiol.* 15: 757–769.
- Armitage, J. (2007). The safety of statins in clinical practice. *Lancet* 370: 1781–1790.
- Bjorkhem-Bergman, L., Lindh, J.D., and Bergman, P. (2011). What is a relevant statin

concentration in cell experiments claiming pleiotropic effects? *Br J Clin Pharmacol* 72: 164–165.

Bratton, L.D., Auerbach, B., Choi, C., Dillon, L., Hanselman, J.C., Larsen, S.D., et al. (2007). Discovery of pyrrole-based hepatoselective ligands as potent inhibitors of HMG-CoA reductase. *Bioorg. Med. Chem.* 15: 5576–5589.

Brown, M.S., and Goldstein, J.L. (2004). A tribute to Akira Endo, discoverer of a “Penicillin” for cholesterol. *Atheroscler. Suppl.* 5: 13–16.

Bruckert, E., Hayem, G., Dejager, S., Yau, C., and Begaud, B. (2005). Mild to moderate muscular symptoms with high-dosage statin therapy in hyperlipidemic patients--the PRIMO study. *Cardiovasc Drugs Ther* 19: 403–414.

Collins, R., Reith, C., Emberson, J., Armitage, J., Baigent, C., Blackwell, L., et al. (2016). Interpretation of the evidence for the efficacy and safety of statin therapy. *Lancet* 388: 2532–2561.

Curtis, M.J., Bond, R.A., Spina, D., Ahluwalia, A., Alexander, S.P.A., Giembycz, M.A., et al. (2015). Experimental design and analysis and their reporting: new guidance for publication in *BJP*. *Br J Pharmacol* 172: 3461–3471.

DeGorter, M.K., Tirona, R.G., Schwarz, U.I., Choi, Y.H., Dresser, G.K., Suskin, N., et al. (2013). Clinical and pharmacogenetic predictors of circulating atorvastatin and rosuvastatin concentrations in routine clinical care. *Circ. Cardiovasc. Genet.*

Deichmann, R., Lavie, C., and Andrews, S. (2010). Coenzyme Q10 and statin-induced mitochondrial dysfunction. *Ochsner J.* 10: 16–21.

Dohlmann, T.L., Morville, T., Kuhlman, A.B., Chrøis, K.M., Helge, J.W., Dela, F., et al. (2019). Statin Treatment Decreases Mitochondrial Respiration but Muscle Coenzyme Q10 Levels Are Unaltered: The LIFESTAT Study. *J. Clin. Endocrinol. Metab.* 104: 2501–2508.

Draeger, A., Monastyrskaya, K., Mohaupt, M., Hoppeler, H., Savolainen, H., Allemann, C., et al. (2006). Statin therapy induces ultrastructural damage in skeletal muscle in patients without myalgia. *J. Pathol.* 210: 94–102.

Fong, C.W. (2014). Statins in therapy: Understanding their hydrophilicity, lipophilicity, binding to 3-hydroxy-3-methylglutaryl-CoA reductase, ability to cross the blood brain barrier



and metabolic stability based on electrostatic molecular orbital studies. *Eur. J. Med. Chem.* 85: 661–674.

Furberg, C.D., and Pitt, B. (2001). Withdrawal of cerivastatin from the world market. *Curr Control Trials Cardiovasc Med* 2: 205–207.

Galiullina, L.F., Scheidt, H.A., Huster, D., Aganov, A., and Klochkov, V. (2019). Interaction of statins with phospholipid bilayers studied by solid-state NMR spectroscopy. *Biochim. Biophys. Acta - Biomembr.* 1861: 584–593.

Gordon, A.M., Homsher, E., and Regnier, M. (2000). Regulation of contraction in striated muscle. *Physiol. Rev.* 80: 853–924.

Hakamata, Y., Nakai, J., Takeshima, H., and Imoto, K. (1992). Primary structure and distribution of a novel ryanodine receptor/calcium release channel from rabbit brain. *FEBS Lett* 312: 229–235.

Inoue, R., Kono, K., Tanabe, M., Maruyama, K., Ikemoto, T., and Endo, M. (2003a). Effect of cerivastatin on Ca<sup>2+</sup> release from the sarcoplasmic reticulum of mouse and rat skeletal muscle fibers. *J Pharmacol Sci* 91: 241p-241p.

Inoue, R., Tanabe, M., Kono, K., Maruyama, K., Ikemoto, T., and Endo, M. (2003b). Ca<sup>2+</sup>-releasing effect of cerivastatin on the sarcoplasmic reticulum of mouse and rat skeletal muscle fibers. *J Pharmacol Sci* 93: 279–288.

Ioannidis, J.P.A. (2014). More than a billion people taking statins? Potential implications of the new cardiovascular guidelines. *JAMA - J. Am. Med. Assoc.* 311: 463.

Istvan, E. (2003). Statin inhibition of HMG-CoA reductase: a 3-dimensional view. *Atheroscler. Suppl.* 4: 3–8.

Istvan, E.S., and Deisenhofer, J. (2001). Structural mechanism for statin inhibition of HMG-CoA reductase. *Science* (80-. ). 292: 1160–1164.

Jacobson, T.A., and Zimmerman, F.H. (2006). Fibrates in Combination With Statins in the Management of Dyslipidemia. *J. Clin. Hypertens.* 8: 35–41.

Kermode, H., Williams, A.J.A.J., and Sitsapesan, R. (1998). The interactions of ATP, ADP, and inorganic phosphate with the sheep cardiac ryanodine receptor. *Biophys. J.* 74: 1296–1304.

Knauer, M.J., Urquhart, B.L., Meyer Zu Schwabedissen, H.E., Schwarz, U.I., Lemke, C.J., Leake, B.F., et al. (2010). Human skeletal muscle drug transporters determine local exposure and toxicity of statins. *Circ. Res.* *106*: 297–306.

Kushnir, A., Todd, J.J., Witherspoon, J.W., Yuan, Q., Reiken, S., Lin, H., et al. (2020). Intracellular calcium leak as a therapeutic target for RYR1-related myopathies. *Acta Neuropathol.* *139*: 1089–1104.

Larsen, S.D., Poel, T.J., Filipski, K.J., Kohrt, J.T., Pfefferkorn, J.A., Sorenson, R.J., et al. (2007). Pyrazole inhibitors of HMG-CoA reductase: an attempt to dramatically reduce synthetic complexity through minimal analog re-design. *Bioorg Med Chem Lett* *17*: 5567–5572.

Laver, D.R. (2001). The power of single channel recording and analysis: Its application to ryanodine receptors in lipid bilayers. In *Clinical and Experimental Pharmacology and Physiology*, pp 675–686.

Liantonio, A., Giannuzzi, V., Cippone, V., Camerino, G.M., Pierno, S., and Camerino, D.C. (2007). Fluvastatin and atorvastatin affect calcium homeostasis of rat skeletal muscle fibers in vivo and in vitro by impairing the sarcoplasmic reticulum/mitochondria Ca<sup>2+</sup>-release system. *J Pharmacol Exp Ther* *321*: 626–634.

Lindsay, C. (2018). Atorvastatin Activates Skeletal RyR1 Channels: Towards Reducing Statin Side-Effects. *Biophys. J.* *114*: 470a.

Lindsay, C., Sitsapesan, M., Chan, W.M., Venturi, E., Welch, W., Musgaard, M., et al. (2018). Promiscuous attraction of ligands within the ATP binding site of RyR2 promotes diverse gating behaviour. *Sci. Rep.* *8*:

Loubinoux, B., Sinnes, J.L., Osullivan, A.C., and Winkler, T. (1995). The Enantioselective Synthesis of Simplified Southern-Half Fragments of Soraphen-A. *Tetrahedron* *51*: 3549–3558.

Maggini, M., Raschetti, R., Traversa, G., Bianchi, C., Caffari, B., Cas, R. Da, et al. (2004). The cerivastatin withdrawal crisis: a ‘post-mortem’ analysis. *Health Policy (New. York).* *69*: 151–157.

Mann, D.M., Woodward, M., Muntner, P., Falzon, L., and Kronish, I. (2010). Predictors of nonadherence to statins: A systematic review and meta-analysis. *Ann. Pharmacother.* *44*:

1410–1421.

McKenney, J.M. (2003). Pharmacologic characteristics of statins. *Clin Cardiol* 26: 11132–11138.

Newman, C.B., Preiss, D., Tobert, J.A., Jacobson, T.A., Page, R.L., Goldstein, L.B., et al. (2019). Statin Safety and Associated Adverse Events: A Scientific Statement From the American Heart Association. *Arter. Thromb Vasc Biol* 39: e38–e81.

Newman, C.B., and Tobert, J.A. (2018). Statin-Related Myopathy and Rhabdomyolysis. In *Endocrine and Metabolic Medical Emergencies*, pp 760–774.

Nishimura, R.A., Otto, C.M., Bonow, R.O., Carabello, B.A., Erwin, J.P., Guyton, R.A., et al. (2014). 2014 AHA/ACC guideline for the management of patients with valvular heart disease: Executive summary :A report of the american college of cardiology/american heart association task force on practice guidelines. *Circulation* 129: 2440–2492.

Oates, J.A., Wood, A.J. j., and Grundy, S.M. (1988). HMG-CoA Reductase Inhibitors for Treatment of Hypercholesterolemia. *N. Engl. J. Med.* 319: 24–33.

Park, W.K.C., Kennedy, R.M., Larsen, S.D., Miller, S., Roth, B.D., Song, Y., et al. (2008). Hepatoselectivity of statins: Design and synthesis of 4-sulfamoyl pyrroles as HMG-CoA reductase inhibitors. *Bioorganic Med. Chem. Lett.* 18: 1151–1156.

Parker, B.A., Capizzi, J.A., Grimaldi, A.S., Clarkson, P.M., Cole, S.M., Keadle, J., et al. (2013). Effect of statins on skeletal muscle function. *Circulation* 127: 96–103.

Pfefferkorn, J.A., Choi, C., Song, Y., Trivedi, B.K., Larsen, S.D., Askew, V., et al. (2007a). Design and synthesis of novel, conformationally restricted HMG-CoA reductase inhibitors. *Bioorg. Med. Chem. Lett.* 17: 4531–4537.

Pfefferkorn, J.A., Song, Y., Sun, K.L., Miller, S.R., Trivedi, B.K., Choi, C., et al. (2007b). Design and synthesis of hepatoselective, pyrrole-based HMG-CoA reductase inhibitors. *Bioorg. Med. Chem. Lett.* 17: 4538–4544.

Raghavan, S., and Samanta, P.K. (2013). Stereoselective synthesis of the C13-C28 subunit of (-)-laulimalide utilizing an  $\alpha$ -chlorosulfide intermediate. *Synlett* 24: 1983–1987.

Rios, E., and Brum, G. (1987). Involvement of dihydropyridine receptors in excitation-

contraction coupling in skeletal muscle. *Nature* 325: 717–720.

Schachter, M. (2005). Chemical, pharmacokinetic and pharmacodynamic properties of statins: An update. *Fundam. Clin. Pharmacol.* 19: 117–125.

Schirris, T.J.J., Renkema, G.H., Ritschel, T., Voermans, N.C., Bilos, A., Engelen, B.G.M. van, et al. (2015). Statin-Induced Myopathy Is Associated with Mitochondrial Complex III Inhibition. *Cell Metab.* 22: 399–407.

Sirvent, P., Mercier, J., Vassort, G., and Lacampagne, A. (2005). Simvastatin triggers mitochondria-induced Ca<sup>2+</sup> signaling alteration in skeletal muscle. *Biochem Biophys Res Commun* 329: 1067–1075.

Sitsapesan, R., Montgomery, R.A., MacLeod, K.T., and Williams, A.J. (1991). Sheep cardiac sarcoplasmic reticulum calcium-release channels: modification of conductance and gating by temperature. *J. Physiol.* 434: 469–488.

Sitsapesan, R., and Williams, A.J.J. (1990). Mechanisms of caffeine activation of single calcium-release channels of sheep cardiac sarcoplasmic reticulum. *J. Physiol.* 423: 425–439.

Stern, R.H., Yang, B.-B., Hounslow, N.J., MacMahon, M., Abel, R.B., and Olson, S.C. (2000). Pharmacodynamics and Pharmacokinetic-Pharmacodynamic Relationships of Atorvastatin, an HMG-CoA Reductase Inhibitor. *J. Clin. Pharmacol.* 40: 616–623.

Suzuki, M., Iwasaki, H., Fujikawa, Y., Sakashita, M., Kitahara, M., and Sakoda, R. (2001). Synthesis and biological evaluations of condensed pyridine and condensed pyrimidine-based HMG-CoA reductase inhibitors. *Bioorganic Med. Chem. Lett.* 11: 1285–1288.

Taha, D.A., Moor, C.H. De, Barrett, D.A., Lee, J.B., Gandhi, R.D., Hoo, C.W., et al. (2016). The role of acid-base imbalance in statin-induced myotoxicity. *Transl. Res.* 174: 140-160.e14.

Tomaszewski, M., Stępień, K.M., Tomaszewska, J., and Czuczwar, S.J. (2011). Statin-induced myopathies. *Pharmacol. Reports* 63: 859–866.

Ueda, P., Lung, T.W.C., Clarke, P., and Danaei, G. (2017). Application of the 2014 NICE cholesterol guidelines in the English population: A cross-sectional analysis. *Br. J. Gen. Pract.* 67: e598–e608.

Vaughan, C.J., and Gotto, A.M. (2004). Update on statins: 2003. *Circulation* 110: 886–892.




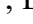
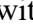

Venturi, E., Lindsay, C., Lotteau, S., Yang, Z., Steer, E., Witschas, K., et al. (2018). Simvastatin activates single skeletal RyR1 channels but exerts more complex regulation of the cardiac RyR2 isoform. *Br. J. Pharmacol.* *175*: 938–952.

Ward, N.C., Watts, G.F., and Eckel, R.H. (2019). Statin Toxicity: Mechanistic Insights and Clinical Implications. *Circ. Res.* *124*: 328–350.

Yamashita, Y., Yasukawa, T., Yoo, W.J., Kitanosono, T., and Kobayashi, S. (2018). Catalytic enantioselective aldol reactions. *Chem. Soc. Rev.* *47*: 4388–4480.

## Figure legends

### Figure 1. The effects of commonly prescribed statins on RyR1 channel activity

(A) The chemical structures of atorvastatin, cervistatin, simvastatin, pravastatin, fluvastatin and rosuvastatin are shown. In each structure, the statin HMG-CoA pharmacophore is indicated in blue. The pharmacophore can interconvert between open and ring-closed forms as illustrated in the inset. (B) Stimulation of [<sup>3</sup>H]ryanodine binding to sheep skeletal muscle SR membrane vesicles by commonly-prescribed statins indicated as a percentage of control binding levels (10  $\mu$ M  $\text{Ca}^{2+}$  as sole activator). Atorvastatin (  ;  $\text{EC}_{50}$  = 0.76  $\mu$ M) cervistatin (  ;  $\text{EC}_{50}$  = 0.42  $\mu$ M) , simvastatin (  ;  $\text{EC}_{50}$  = 0.70  $\mu$ M), pravastatin (  ;  $\text{EC}_{50}$  = 0.44  $\mu$ M), fluvastatin (  ;  $\text{EC}_{50}$  = 0.42) and rosuvastatin (  ;  $\text{EC}_{50}$  = 0.49  $\mu$ M) are shown. Mean  $\pm$  SEM; n = 5; where error bars are not visible, they are within the symbol.

### Figure 2. The effects of atorvastatin and cervistatin on RyR1 single channel function

Representative sheep skeletal RyR1 single channel fluctuations in the presence of 10  $\mu$ M cytosolic  $\text{Ca}^{2+}$  alone (top trace) and after addition of cytosolic atorvastatin (A) or cervistatin (B) as indicated (middle traces) and after washout of the cytosolic chamber to control conditions (bottom trace). O and C indicate the open and closed channel levels respectively. The  $P_o$  above each trace refers to the value determined over 3 min. (C) Concentration-response relationships for the activation of RyR1 channels by cytosolic atorvastatin and cervistatin. Mean  $\pm$  SEM; n = 8-22. (D) Mean  $P_o$  values for RyR1 channels in the presence 10  $\mu$ M  $\text{Ca}^{2+}$  and after addition of atorvastatin (concentrations indicated) for RyR1 channels derived from sheep (blue), rabbit (orange) and mouse (green) skeletal muscle, respectively.

### Figure 3. The $\text{Ca}^{2+}$ -dependency of statin RyR1 activity.

Representative sheep skeletal muscle RyR1 single channel fluctuations at sub-activating [ $\text{Ca}^{2+}$ ] < 1 nM  $\text{Ca}^{2+}$  (top trace) are shown, and after addition of cytosolic atorvastatin (A) or cervistatin (B) as indicated. Note the difference in concentrations between atorvastatin and cervistatin. O and C indicate the open and closed channel levels, respectively. The  $P_o$  above each trace refers to the value determined over 3 min. (C) Mean  $P_o$  values for RyR1 channels before (white bars) and after (pink bars) addition of 100 nM cervistatin at the free [ $\text{Ca}^{2+}$ ] indicated. Mean  $\pm$  SEM; \* $p$  < 0.05 relative to respective controls; n = 6 – 11. (D) Representative sheep skeletal muscle RyR1 single channel fluctuations under control

conditions (100 nM cytosolic  $\text{Ca}^{2+}$ , 1 mM free  $\text{Mg}^{2+}$  and 5 mM ATP) (top trace) and after addition of cytosolic cerivastatin as indicated. O and C indicate the open and closed channel levels, respectively. The Po above each trace refers to the value determined over 3 min. **(E)** Mean RyR1 Po values under control conditions (100 nM cytosolic  $\text{Ca}^{2+}$ , 1 mM free  $\text{Mg}^{2+}$  and 5 mM ATP) and after the subsequent addition of cerivastatin as indicated. Mean  $\pm$  SEM; \* $p < 0.05$ ;  $n = 15 - 32$ .

**Figure 4. Synthesis of the statin pharmacophore and its effect on RyR1 activity.**

**(A)** The chemical structure of atorvastatin indicating the statin HMG-CoA pharmacophore (blue) and its comparison to the minimal pharmacophore (inset). **(B)** Synthetic route to statin minimal pharmacophores **(R)-1** and **(S)-1**. Reaction conditions: (i) NaH, TBDPSCl, THF, RT, 16 h; (ii)  $(\text{COCl})_2$ , DMSO,  $\text{Et}_3\text{N}$ ,  $-78^\circ\text{C}$ , 1hr; (iii) **4**,  $n\text{Bu}_2\text{BOTf}$ ,  $\text{CH}_2\text{Cl}_2$ ,  $-78^\circ\text{C}$  to  $0^\circ\text{C}$ , 2.5 h; (iv) HF/pyr, THF, RT, 3 h; (v)  $\text{Et}_3\text{N}$ ,  $\text{CH}_2\text{Cl}_2$ , RT, 48 h. **(C)** Stimulation of  $[^3\text{H}]$ ryanodine binding to sheep skeletal SR membrane vesicles by **(R)-1**, **(S)-1** and their respective sodium salts, indicated as a percentage of control binding levels. Cerivastatin data from Figure 1(B) is indicated in pink for comparison. Mean  $\pm$  SEM;  $n = 5$ ; where error bars are not visible, they are within the symbol.

**Figure 5. Structure-activity relationship for the activation of RyR1 by atorvastatin analogues.**

**(A)** Chemical structures of atorvastatin analogues **P1-P16**, their experimentally determined  $\text{IC}_{50}$  values for *in vitro* HMG-CoA inhibition ((Suzuki et al., 2001; Bratton et al., 2007; Larsen et al., 2007; Pfefferkorn et al., 2007b, 2007a; Park et al., 2008)) and the maximum stimulation (RyR1 activation) or inhibition (RyR1 inhibition) of  $[^3\text{H}]$ ryanodine binding to sheep skeletal muscle SR membranes. RyR1 activators are shown in blue, RyR1 inhibitors in red and those compounds with no effect on RyR1 activity are shown in white. **(B)** Stimulation of  $[^3\text{H}]$ ryanodine binding for compounds **P1-P16** at 100 nM, relative to control binding levels. 100 nM cerivastatin and 100 nM atorvastatin are also shown for comparison. Mean  $\pm$  SEM;  $n = 5$ . **(C)** Line graphs of the relationship between ability to stimulate  $[^3\text{H}]$ ryanodine binding to sheep skeletal muscle SR membranes for activators and inhibitors relative to control binding levels. Compounds with no effect on RyR1 within the given range of concentrations are not shown. The lines have no theoretical significance and are shown for ease of comparison only. Error bars are not shown for clarity. The symbols are shown in the adjacent legend. **(D)** Concentration-response relationships for P1, P5, P6 and P8 relative to control binding levels

are shown. To illustrate the inactivity of these compounds, the cerivastatin data from Figure 1 is also shown (Mean  $\pm$  SEM; n = 6).

**Figure 6.**

General structure-activity relationships showing the structural features which influenced RyR1 activity. Panels show how the identity of the R<sub>1</sub> group corresponds with the ability to activate or inhibit RyR1 or lacks ability to affect RyR1 Po as indicated. Compound numbers are also indicated below each structure.